ZIBELINE INTERNATIONAL PUBLISHING

Earth Sciences Malaysia (ESMY)

DOI: http://doi.org/10.26480/esmy.02.2020.140.145

ISSN: 2521-5035 (Print)
ISSN: 2521-5043 (Online)
CODEN: ESMACU

CrossMark

RESEARCH ARTICLE

ASSESSING THE SUSCEPTIBILITY OF STRUCTURAL COLLAPSE USING SEISMIC REFRACTION METHOD

Mfoniso U. Aka[a], Okechukwu E. Agbasi[b*], Johnson C. Ibuot[a], Mboutidem D. Dick[c]

[a]Department of Physics and Astronomy, University of Nigeria, Nsukka, Nigeria
[b]Department of Physics, Micheal Okpara University of Agriculture, Umudike, Nigeria
[c]Department of Science Laboratory, Akwa Ibom State Polytechnic, Ikot Osurua, Nigeria
**Corresponding Author's Email: agbasi.okechukwu@gmail.com*

ARTICLE DETAILS

Article History:

Received 01 August 2020
Accepted 03 September 2020
Available online 10 September 2020

ABSTRACT

Seismic refractive survey is a very important geophysical technique used to investigate the characteristics of the subsurface. The rate of building collapse has demanded the acquaintance about the structure of the subsurface especially in area where lands are recovered from water bodies for the aim of building. This paper presents the technique used in determining the thickness of the overburden for quarry prospecting using a geophysical method called as seismic refraction method. Seismic refraction method was used to delineated two distinct layers with the first layer having a weak and incompetent parameter values. The result revealed that the first layer is composed of unconsolidated formation of soft geomaterials and peaty clay that depict the lower values of parameters. This layer is underlain directly by clay, wet sand and sandy clay of soft and weak incompetent consistencies to a depth of 7 m in the subsurface. The second layer was found to have higher parameters than the first layer. The second layer revealed that the geologic formation composed of dry sand and sandy clay of fair to good competent. The geologic formation in the second layer was found to be more competent than the first layer with high allowable capacity and low ultimate failure potential. Geologically, the composition of the first layer is more recent in age of deposition than the second layer, characterized by unconsolidated geologic formation.

KEYWORDS

Allowable Capacity, Geomaterials, Structural Failure, Subsurface Geophysics.

1. INTRODUCTION

Seismic surveys are commonly used around the world for creating a clear picture of the geology below the surface of the earth. The method of seismic refraction is one of the seismic techniques that is commonly used to evaluate soil and rock characteristics (Adegbola et al., 2013; Ayolabi et al., 2009). The application of seismic refraction is to evaluate rock competence for engineering applications, depth to bedrock, groundwater exploration, crustal structure and tectonics (Kilner et al., 2005; Ochuko, 2013; Varughese et al., 2011; Chiemeke and Aboh, 2012). The seismic refraction method is based on calculating the travel time of seismic waves refracted at the interfaces between different velocity layers of the subsurface (Ayolabi et al., 2009). Using explosives, hammer blast, dropped weight or an elastic wave generator (Igboekwe and Ohaegbuchu, 2011), the seismic signal is fed into the subsurface through a shot point. The generated energy either travels directly through the upper layer (direct arrivals), or travels down the different layers before returning to the surface (refracted arrivals). The energy is then measured at regular intervals on the surface at a series of receivers called geophones (Anomohanran, 2012). At a certain distance from the point of shooting, known as the cross over stage, the refracted signal is detected at the geophones (arriving before the direct arrival) as a first-arrival signal. All compressional waves (P-waves) providing interface depth information and Shear waves (S-waves) providing additional details on the engineering properties of the waves the seismic refraction method can use subsurface media (Ahmed et al., 2012).

The seismic approach relies on the propensity to increase with depth of acoustic velocities, which often renders it insensitive to low velocity layers in the subsurface. Based on the field data study, the seismic surveyor draws a profile showing the subsurface thickness and a clear understanding of what materials they consist of (Ayolabi et al., 2009; Varughese et al., 2011; Igboekwe and Ohaegbuchu, 2011; Ahmed et al., 2012; Okiongbo et al., 2011). Seismic refractive survey uses the critical refraction method to infer interface depths and velocities of layers. Usually the data are plotted as time-distance curves and then presented to different interfaces as cross-sectional plots representing P-wave path, velocities, and depths.

Structural failure in Nigeria has become main anxiety of people as it affects the life and properties. It therefore, poses a serious challenge to subsurface-geophysicists, engineers, building consultants, governments, landlords and other land users. Typical example of collapsed building is the Reigners Bible Church Uyo, Akwa Ibom State that claim much lives and properties worth billions of naira as shown in Figures 1 and 2. This collapse has been accredited to a numerous factor such as insufficient information about the soil subsurface, elastic, bearing capacity, poor

Quick Response Code	Access this article online	
	Website: www.earthsciencesmalaysia.com	**DOI:** 10.26480/esmy.02.2020.140.145

engineering and foundation design of the materials" (Fatoba et al., 2010; George et al., 2010; Zhang and Toksoz, 1998). In order to avert forfeiture of cost in the cases of structural failure, it is important to understand the subsurface characteristics and the geologic condition of the soil before there are recommended for construction purposes (Coker et al., 2013; Oyedele et al., 2011; Aka and Umoh, 2013). Foundation is the supportive base of the structure which forms the boundary diagonally which the loads are conveyed to the fundamental rock. Thus, if the structural loads are conveyed to the near surface earth a near superficial foundation is formed which includes; mat foundation and spread footing (George et al., 2010). However, in order to assess the subsurface, seismic refraction method was used in this study to evaluate the susceptibility of the near surface and correlate the result with lithology of the area in order to evaluate the depth to the most capable layer in the area of study (Aka and Umoh, 2013).

The seismic refraction technique is highly useful in many applications such as engineering, environmental, groundwater, hydrocarbon and mineral exploration to describe the subsurface structure and geological condition (Usman et al., 2018; Ugwu, 2009; Dutta, 1984). This technique splits the subsurface structure into diverse layers and it gives evidence on the engineering parameters of each layer and their thicknesses (Aka et al., 2018). Seismic refraction method functions on the principle that the swiftness of proliferation of seismic energy fluctuates with the medium of propagation. Seismic refraction introduces primary (P) and secondary (S) waves, these waves generated by the energy sources and perceived by collections of geophone and seismograph plotter in the layered outlines for near surface profile data. Measured velocities (P and S waves) are evaluted along with elastic, bearing capacity and engineering properties (Grant and West, 1965; Kumar, 2003; Ulugergerli and Uyanik, 2007). The rate of building collapse has demanded the acquaintance about the structure of the subsurface especially in area where lands are recovered from water bodies for the aim of building. These sites are known to comprise geologic formations which are mechanically unbalanced for locating an engineering structure (Egwonwu and Sole, 2012; Agoha et al., 2015). Building catastrophe ranges from settlement, upthrust and total collapse as shown in Figures 1 and 2 respectively.

Figure 1: The collapse Reigners Bible Church structures

Figure 2: Middle view of the collapsed Reigners Bible Church

2. Geology of The Study Area

Uyo is found in South-South region of Nigeria and is the capital of Akwa Ibom State. It is located within Latitudes $4^0 57^1$N to $5^0 30^1$N and Longitudes $7^0 56^1$E to $7^0 60^1$E with an elevation of 196 m above the sea level. It is bordered on the south by Nsit Atai, Nsit Ibom and Etinan Local Government Area, on the west by Abak Local Government Area, on the North by Ikono and Itu Local Government Areas of Akwa Ibom State with a total area of 255.9 km^2 as shown in Figure 3. It is underlain by sedimentary formation of late tertiary and Holocene ages within the equatorial rain forest belt, which is a tropical zone and home to vegetation of green foliage of trees, shrubs and oil palm trees. It is a tourism attraction center which includes: Ibom plaza park, Le meridian hotel and Golf resort. Also, home of the Ibom E-Library, a world-class information and research Centre. The Uyo Local government Area has three distinct vegetation zones and two seasons: salty water wetland forest, fresh water wetland forest and rain forest; rainy and dry seasons.

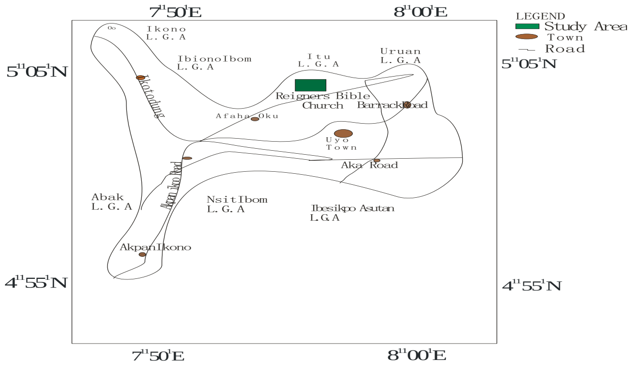

Figure 3: Map of uyo local government area showing the study area and its environment

3. Theory

When seismic refraction source is shot the seismic signal is generated, a series of geophone laid receive the indication in a straight line along the surface, recorded on the seismograph and displaced on the screen. The refracted arrival times (t) of P and S waves are measured as a function of the distance (x) from the seismic source point, the seismic velocity (V_p) of the Primary wave and (V_s) of the Secondary wave of the underlying soil or rock are calculated as the reciprocal of the slope by plotting the first arrival time at each geophone against the distance from the seismic source (Aka and Umoh, 2013; Usman et al., 2018). The reciprocal of the gradient of V_1 gives the velocity of the first layer while the slope of V_2 gives the velocity of the second layer (Akpan and Okwueze, 2006; Atat et al., 2012). Elastic properties; Young modulus, shear modulus, Lames constants and Poisson's ratio, could be used to obtain soil properties. Bearing capacity: allowable and eventual bearing capacity and engineering properties: material index, concentration index, density gradient and stress ratio (Zhang and Toksoz, 1998; Usman et al., 2018; Dutta, 1984).

3.1 Shear Modulus

Shear Modulus (μ) is calculated using equ. 1

$$\mu = \frac{E}{2(1+\sigma)} \tag{1}$$

3.2 Young modulus

Young modulus (E) is calculated using equ. 2

$$\mathrm{E} = \rho \left[\frac{3V_P^2 - 4V_S^2}{\left(\frac{V_S}{V_P}\right)^2 - 1} \right] \tag{2}$$

P is the density of the sample layers.

3.3 Poisson ratio

Poisson ratio (σ) is calculated using equ. 3

$$\sigma = \frac{1}{2}\left[1 - \frac{1}{\left(\frac{V_S}{V_P}\right)^2 - 1} \right] \tag{3}$$

3.4 Lame's constant

Lame's constant (λ) is calculated using equ. 4

$$\lambda = \frac{\sigma E}{(1+\sigma)(1-\sigma)} \quad (4)$$

3.5 Ultimate bearing capacity

Ultimate bearing capacity (q_f) is calculated using equ. 5

$$q_f = \frac{4\gamma V_S}{40} \quad (5)$$

$$\gamma = \gamma_0 + 0.002V_p \quad (6)$$

γ is the unit weight of the soil, γ_0 = 16 KN/m^3 which is the average unit weight of loose soil.

3.7 Allowable bearing capacity

Allowable bearing capacity (q_a) calculates the bearing heaviness that will cause acceptance reimbursement of the structure against unpredictability due to shear failures as expressed in equ. 7

$$q_a = \frac{q_f}{n} \quad (7)$$

Where n = 4.0 for soil, which is the factor of safety.

3.8 Material Index

Material Index (V_1) measures the material property or a combination of material properties between a constraint and function of the material properties that primes to a specific performance index of material properties. It is expressed as shown in equ. 8

$$V_1 = \frac{3-(V_P/V_S)^2}{(V_P/V_S)^2-1} \quad (8)$$

3.9 Stress Ratio

Stress Ratio (S_1) measures ultimate strength of the engineering material to the allowable stress. It also chronicles the quantity of deformation at discrete intermissions of tensile or compressive loading. It is expressed as shown in equ. 9

$$S_1 = 1-2(V_S/V_P)^2 \quad (9)$$

3.10 Concentration Index

Concentration Index (C_1) measures the concentration of the load and soil strength which describe the magnitude of the shear stress that a soil can sustain as a result of friction and interlocking of the soil. It is expressed as shown in equ. 10

$$C_1 = \frac{3-4\left(\frac{V_S^2}{V_P^2}\right)}{1-2\left(\frac{V_S^2}{V_P^2}\right)} \quad (10)$$

3.11 Density Gradient

Density Gradient (D_1) measures the spatial variation in the density of engineering material which varies with temperature and pressure. It is expressed as shown in equ. 11

$$D_1 = \left[\left(\frac{3}{V_P^2}\right)-\left(\frac{4\mu}{E}-1\right)\right] \quad (11)$$

4. METHODOLOGY

Profiling of seismic refraction were surveyed to obtain adequate data for this study. Each profile length stretches 5 to 60 m, inter-geophone spacing of 5 m was used and the shot-to-first geophone spacing was also 5 m as shown in Figures 4 and 5. A total number of 12 P-waves and 12 S-waves geophones were used for forward and reverse shooting on every 60 m profiles length. Two (2) shots were recorded at each location with 2 stacks per shot location to obtain P wave, while four (4) were recorded at each location with 2 stacks per shot location to obtain S wave.

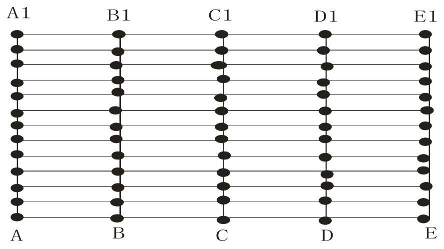

Figure 4: Five seismic refraction survey layouts

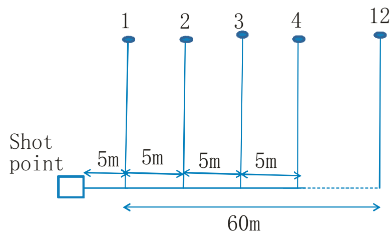

Figure 5: Geophones field setup

For data acquisition the following was used, 12 channels ES 30000s Seismogram; 12 kg sledgehammer; metal plate 4 by 6cm; electrical cables and 48Hz frequency geophones. The density values for the two layers were obtained in the laboratory of collected samples from outcrops. From this seismic refraction method, the refracted arrival times of the recorded signal were picked using Seis Imager software packages of Pickwin and IX-Refrax and plotted as T-X graph showing two velocity layers (V_1 and V_2). The reciprocal of the slope of V_1 gives the velocity of the first layer while the slope of V_2 gives the velocity of the second layer. This value of the two velocities was used to determine other related parameters and state of stress of the soil for the two layers using theories of Eqns. 1 to 11 and Figures. 6 and 7 respectively.

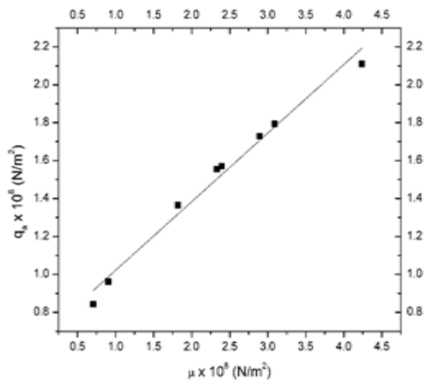

Figure 6: A plot of q_a x 10^8(N/m^2)against µ x10^8 (N/m^2) for layer 1

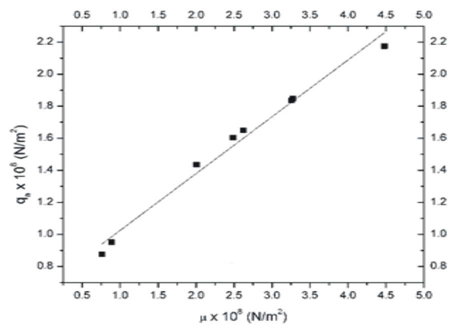

Figure 7: A plot of q_a x 10^8(N/m^2)against µ x10^8 (N/m^2) for layer 2

5. RESULT AND DISCUSSION

Refracted travel times of all recorded traces were investigated using seis

Imager packages of Pickwin and IXrefract software. The seismic tomography section discovers two geologic layers in the study area. That is, layers 1 and 2. The P-wave velocity, first layer (500.4 to 901.2 m/s); second layer (720 and 1010.3m/s). The S-wave velocity, first layer (400.0 and 720.5 m/s); second layer (510.0 and 901.2 m/s). Other parameters were determined as shown in "Table 1". In layer 1: Poisson ratio ranged from 1.49 to 1.99, Young's modulus ranged from between -425.1 to -2021.1 KN/m², Lames constant ranged from 245.8 to 313.8 KN/m², Shear modulus ranged from -613.1 to -2518.7KN/m², Ultimate capacity ranged from 680.0 to 1282.7 N/m², Allowable capacity ranged from 170.0 to 320.7 N/m², Material index ranged from 0.97 to 2.97, Concentration index -1.03 to 132.8, Density gradient ranged from -3.98 to -4.99 and Stress ratio ranged from 0.007 to -0.16. In layer 2: Poisson ratio ranged from 1.36 to 2.94, Young's modulus ranged from between 240.5 to 1597.7 KN/m², Lames constant ranged from -108.5 to 965.8 KN/m², Shear modulus ranged from 432.9 to 3153.1 KN/m², Ultimate capacity ranged from 102 to 180.24 N/m², Allowable capacity ranged from 255.0 to 450.6 N/m², Material index ranged from 0.43 to 6.97, Concentration index 0.09 to 7.99, Density gradient ranged from -3.71 to -6.89 and Stress ratio ranged from -1.51 to -3.80 as shown in "Table 2" respectively. Depths and thickness (0.0 – 5.0 m; 5.0 m) for the topsoil while the second layer (5.5 – 13.0 m; 7.5 m). Geotechnically, the geologic strata with complex values of constraints are considered for engineering construction purposes as observed in the second layer. The result revealed that the first layer is composed of unconsolidated formation of soft geomaterials and peaty clay that depict the lower values of parameters. This layer is underlain directly by clay, wet sand and sandy clay of soft and weak incompetent consistencies to a depth of 7 m in the subsurface. The second layer was found to have higher parameters than the first layer. The second layer revealed that the geologic formation composed of dry sand and sandy clay of fair to good competent. The geologic formation in the second layer was found to be more competent than the first layer with high allowable capacity and low ultimate failure potential. Geologically, the composition of the first layer is more recent in age of deposition than the second layer, characterized by unconsolidated geologic formation. The weak and incompetent geologic formation observed in the first layer shows that, there was no direct pressure of the geologic formation on top of the first layer that festinate the consolidation of the soil deposit. However, the second layer was found to be composed of fair to good consolidated geological formation than the first layer, based on the age of deposition which compressed by the presence of other recent deposit lying on it. The pressure exerted on the second layer by other geological formation lying on it helped to improve its engineering stability. Moreover, the depth to the most competent geologic formation was found in the second layer to be ranged from 5.5 to 13.0 m with the thickness of 7.5 m corresponding to consolidated layer in the subsurface. The velocity of S waves is inversely proportional to travel times because of formation, fluid typing, modulus and rock density. The allowable bearing capacity was plotted with shear modulus which shows a direct relationship amongst the parameters as shown in Figures 6 and 7. The slope of the plots in Figure 7 shows dimensionless constants which give the coefficients of elastic deformation of the near surface cause by load imposed on the near surface.

Table 1: Summary of measured and elastic parameters

Locations	Layers	V_P(m/s)	V_S(m/s)	Σ	E(KN/m²)	λ (KN/m²)	γ(KN/m³)	μ(KN/m²)
A	1	550.5	420.2	1.698	-670.8	604.8	17.10	-904.9
	2	790.2	510.0	1.357	-249.8	402.8	17.58	-294.4
B	1	600.2	489.5	1.993	-503.9	337.9	17.20	-754.2
	2	825.5	720.6	2.601	240.5	108.5	17.65	433.0
C	1	500.4	400.0	1.885	-425.1	313.8	17.01	-61.3I
	2	720.0	590.5	2.027	-857.6	559.0	17.44	-129.8
D	1	852.5	600.5	1.492	-202.1	245.8	17.71	-251.8
	2	1000.2	825.0	2.064	-15.25	965.8	18.01	-233.8
E	1	901.2	720.5	1.886	-137.7	101.6	17.80	-137.7
	2	1010.3	901.2	2.947	159.8	612.6	18.02	315.3

Figures 8 to 13 show the model dispersal of elastic parameters, allowable and engineering parameters for the two layers. The 2-D model in Figures 8 and 9 shows a continuous increment in the shear modulus in the east – west trend in layer 1 and north – west in layer 2 and decrease in the east trend. Figures 10 to 13 show an increase of allowable bearing capacity and material index in the east trend and decrease in the west trend in layers 1 and 2. This inclination displays that low allowable and elastic parameters is allied with zone that area highly drained with water whereas high bearing and elastic parameters are unsaturated with water. However, in 3-D model as shown in Figure 14, the location of high values of allowable and material index in the layer 1 adapts to the location noticed in layer 2. These results prove uniform alliance trends from low to high value with depth in layer 1 and 2. This conformism reveals the exceptionality of the method used in inspecting the near surface structures. On the other hand, this study revealed that any study area having similar geology formation, the second layer portion of the subsurface should be considered for engineering construction that will provide safety and stand the test of time.

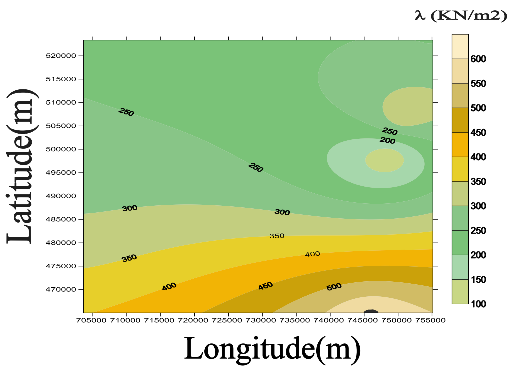

Figure 8: 2-D contour map showing the distribution of λ (KN/m²) in layer 1

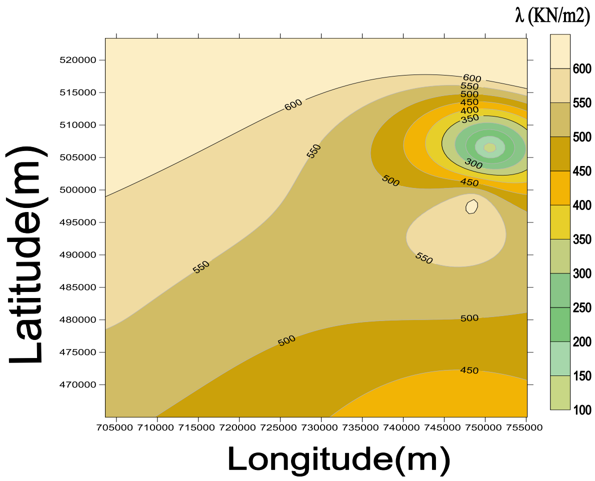

Figure 9: 2-D contour map showing the distribution of λ (KN/m²) in layer 2

Table 2: Summary of bearing and engineering parameters

q_a (N/m²)	q_f (N/m²)	V_1	C_1	D_1
17.96	718.5	1.792	-4.051	-4.396
25.5	10.20	0.428	7.992	-3.714
21.05	842.0	2.973	-1.03	-4.986
36.03	144.1	4.403	0.092	-6.202
17.01	680.03	2.540	-1.598	-4.770
29.53	118.21	3.109	-0.896	-5.055
26.58	106.31	0.992	1.328	-3.985
41.25	165.00	3.257	-0.77	-5.129
32.07	128.27	2.543	-1.592	-4.772
45.06	180.24	6.789	0.309	-6.894

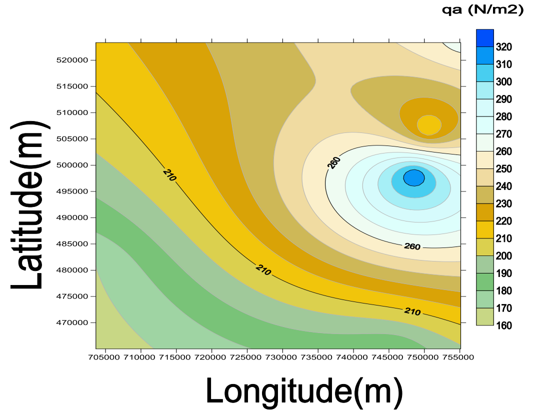

Figure 10: 2-D contour map showing the distribution of q_a (N/m^2) in layer 1

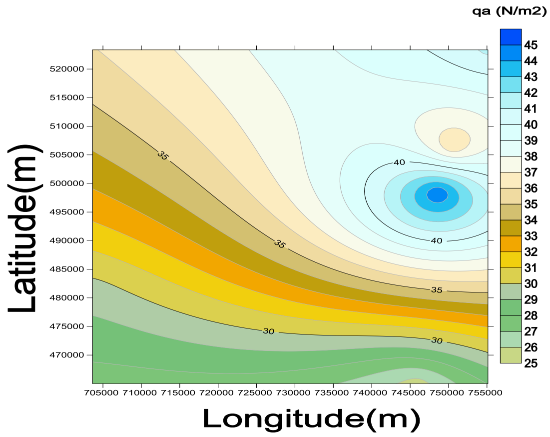

Figure 11: 2-D contour map showing the distribution of q_a (N/m^2) in layer 2

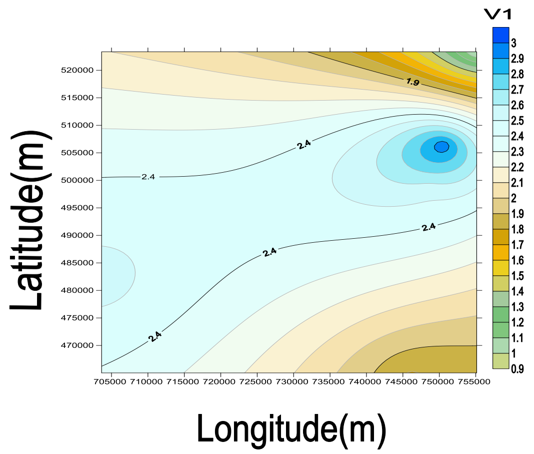

Figure 12: 2-D contour map showing the distribution of V_1 in layer 1

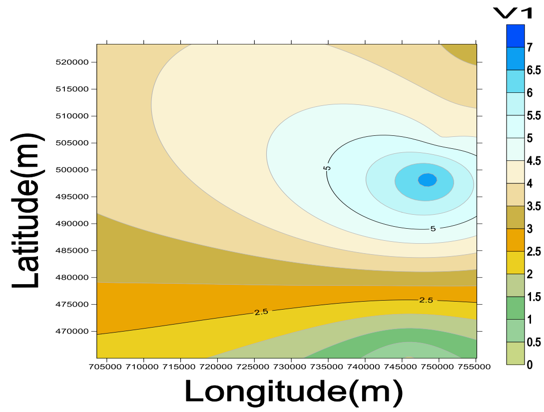

Figure 13: 2-D contour map showing the distribution of V_1 in layer 2

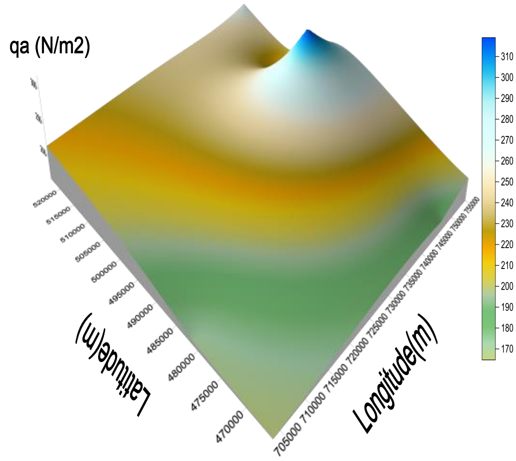

Figure 14: 3-D model showing the distribution of qa (N/m^2) in layer 1

6. Conclusions

The method of seismic refraction near surface was used to assess the vulnerability of the collapse of buildings. Seismic refraction is a useful and reliable geophysical method for geophysical and engineering study of near-surface conditions. This could be seen in its ability to recognise frail and incompetent ultimate potential of bearing and frail layers of engineering that do not help sustainable engineering. It is worth concluding that the engineers and road builders will make use of the inferred near-surface elastic, bearing capability and engineering parameters to create buildings / road that will stand the test of time. In addition, weak and inept sub-surface elastic, bearing and engineering geomaterials, which are the main cause of building / road failure in the region, must be removed and replenished with good engineering geomaterials such as laterite for better optimized near-surface characterisation for engineering projects. Description of the strengths of elastic, bearing ability and engineering parameters show fine, strong, and compressed rock basement. This will support structural works that would withstand the burdens on the structural works, minimizing the destruction of life and property and fast track the area's rapid economic development.

Acknowledgment

We are grateful to all qualified cadres during the field work, reviewers and editors whose tolerance and constructive comments contributed to the success of this manuscript.

References

Adegbola, R.B., Ayolabi, E.A., Allo, W. 2013. Subsurface Characterization Using Seismic Refraction and Surface Wave Methods: A Case of Lagos State University, Ojo, Lagos State. Arabian Journal of Geoscience 6(12), 4925–4930.

Agoha. C., Opara, A.I., Okereke, C.N., Onwubuariri, C.N., Emberga. T.T., Inyang, G.E., Ugwuegbu, I.E., Chilaka, J.C., 2015. Weathered Layer Determination and its effects on Engineering Structures. A case study of parts of Niger Delta, Nigeria. World Journal of Environmental Engineering, 3(2), 40-51.

Ahmed, I.I., Osazuwa, I.B., Lawal, K.M. 2012. 2-D Seismic Refraction Tomography Investigation of a sewage treatment site", Journal of Environmental and Earth Science, IISTE, 2(10), 1 – 14.

Aka, M.U., Okeke, F.N., Ibout, J.C., Obiora, D.D. 2018. Geotechnical Investigation of Near-surface Structures using Seismic Refraction Techniques in parts of Akwa Ibom State, Southern Nigeria. Modelling Earth System Environment. 4, 451-459.

Aka, M.U., Umoh, J.A. 2013. Determination of Weathering Thickness and Velocity of the Near Surface Layers using Uphole Seismic Refraction Survey. Proceeding International Conference for Research, Innovation and Sustainable. Development, 4(1), 10-17.

Akpan, A.E., Okwueze, E.E. 2006. Shear Wave Observation in Seismic Refraction Prospecting. Journal of Mining and Geology, 24 (2), 1-2.

Anomohanran, O. 2012. Geophysical interpretation of seismic reflection data obtained from Umureute and Amiynaibo area of Delta state. Nigeria. Nigerian Journal of Science and Environment 11: 148-153.

Atat, J.G., Akpabio, G.T., George, N.J., Umoren, E.B. 2012. Geophysical Assessment of Elastic Constants of Top Soil using Seismic Refraction Compressional and Shear wave Velocity in the Eastern Niger Delta, Nigeria. International Journal of Modern Applied Physics, (1), 7-19.

Ayolabi, E.A., Adeoti, L., Oshinlaja, N.A., Adeosun, I.O., Idowu, O.I. 2009. Seismic refraction and resistivity studies of part of Igbogbo township, south-west Nigeria. Journal of Scientific Research and Development. 11, 42-61.

Chiemeke, C.C., Aboh, H.O. 2012. Delineation of aquiferous layers within the basement complex using joint inversion of seismic refraction tomography and high-resolution 3D seismic reflection survey. Archies of Applied Science Research. 4, 400-405.

Coker, J.O., Makinde, V., Mustapha, A.O., Adesodun, J.K. 2013. The Application of Geophysical Methods in Foundation Failure Investigation. A case study of Metro Hostel Camp Area, Abeokuta, South Western Nigeria. Nature and Science, 11(11), 13-18.

Dutta, N.P., 1984. Seismic Refraction Method to study the foundation Rock of Dam, Geophysics Prospecting. 32, 1103-1110.

Egwonwu, G.N., Sole, P.O. 2012. Geophysical Investigation of Foundation Failure of a Leaning Superstructure in Zaria Area, Northern Nigeria. Research Journal in Engineering and Applied Sciences, 1(2): 110- 116.

Fatoba, J.O., Alo, J.O., Fakeye, A.A. 2010. Geoelectric imaging for foundation failure investigation at Olabisi Onabanjo University mini campus, Ago Iwoye, Southwestern Nigeria. Journal of Applied Science and Research, 6(12), 2192-2198.

George, N.J., Akpan, A.E., George, A.M., Obot, I.B. 2010. Determination of Elastic Properties of the Overburden Materials in parts of Akamkpa, Southeastern, Nigeria using Seismic Refraction Studies. Archives of Physics Research, (2), 58 – 71.

Grant, F.S., West, G.F. 1965. Interpretation Theory in Applied Geophysics. New York: McGraw Hill. Textbook, 8 -12.

Igboekwe, M.U., Ohaegbuchu, H.E. 2011. Investigation into the weathering layer using up-hole method of seismic refraction. Journal of Geology and Mining Research. 3(3), 73-86.

Kilner, M., West, L.J., Murray, T. 2005. Characterisation of glacial sediments using geophysical methods for groundwater source protection. Journal of Applied Geophysics 57(4), 293-305.

Kumar, J. 2003. Seismic Bearing Capacity Factors for Spread Foundations, Banabara India Geotechnique 3(53), 363-369.

Ochuko, A. 2013. Seismic refraction method: A technique for determining the thickness of stratified substratum. American Journal of Applied Sciences 10(8), 857-862.

Odumodu, C.F.R., Ezeh, M.O. 2014. Weathering layer Delineation in an X-Field in the Niger Delta Basin of Nigeria. The Uphole Data Acquisition Technique. Journal of Earth Science and Geotechnical Engineering, 4(3), 115- 130.

Okiongbo, K.S., Akpofure, E., Odubo, E. 2011. Determination of aquifer protective capacity and corrosivity of near surface materials in Yenagoa city, Nigeria. Research Journal of Applied Sciences, Engineering and Technology. 3(8), 785-791.

Oyedele, K.F., Oladele, S., Adedoyin, O. 2011. Application of Geophysical and Geophysical Methods to Site Characterization for Construction Purposes at Ikoyi, Lagos, Nigeria. Journal of Earth Sciences and Geotechnical Engineering, 1(1), 87- 100.

Ugwu, S.A. 2009. Determination of depth to bedrock in Afikpo syncline of the Benue Trough, Nigeria, using seismic refraction methods. Scientia Africana 7(2), 32 – 41.

Ulugergerli, E.U., Uyanik, O. 2007. Statistical Correlation between Seismic Wave Velocities and SPT Blow Counts and the Relative Density of Soils. Journal of Testing and Evaluation. 35(2), 187-191.

Usman, D.A., Daniel, O., Francisca, N.O. Johnson, I. 2018. Investigation of groundwater potential of southern Paiko, northcentral Nigeria, using seismic refraction method. Modeling Earth Systems and Environment 4(25), 555 – 564.

Varughese, A., Kumar, P., Kumar, N. 2011. Seismic refraction survey a reliable tool for subsurface characterization for hydropower projects. Proceedings of Indian Geotechnical Conference, Dec. 15-17, Kochi. 137-139.

Zhang, J., Toksoz, M.N. 1998. Nonlinear Refraction Travel Time Tomography. Geophysics 63, 1726-1737